Maria Carmela DI PIAZZA,Antonella RAGUSA, Gianpaolo VITALE

Consiglio Nazionale delle Ricerche- ISSIA

Magnetic material performance of transformers in common mode active EMI filters for bearing current suppression

Abstract. *This paper analyses the performance of two magnetic materials used in the active filters for Common Mode (CM) electromagnetic interference (EMI) reduction in induction motor drives. In particular, active filters based on CM voltage compensation, very useful in bearing current suppression, are considered. The magnetic material is exploited for the core of the common mode transformer (CMT) that it is a crucial part of such devices because it performs the injection of the compensation voltage into the power connections between the inverter and the motor. The issues regarding the choice of the CMT core magnetic material and the windings design are discussed. The problem of the magnetic saturation, related to the desired high power/weight ratio is investigated. Furthermore, the power losses in the magnetic material under non-sinusoidal supply condition are evaluated through a suitable measurement system. A comparison of two CMTs, realized with ferrite and with nanocrystalline material cores, respectively, which are designed to perform the same filtering effect, is presented.*

Streszczenie. *W artykule przedstawiono analizę właściwości dwóch materiałów magnetycznych stosowanych w aktywnych filtrach EMI. Przedstawiono zalecenia dotyczące doboru materiału (głównie indukcji nasycenia) jak i konstrukcji dławików i transformatorów. Zmierzono także straty mocy w warunkach zasilania niesinusoidalnego. Porównano dwa materiały – ferryty i materiały nanokrystaliczne. (**Właściwości materiałów magnetycznych stosowanych w aktywnych filtrach EMI**)*

Keywords: Transformer cores, soft magnetic materials, losses, EMI active filters, induction motor drives
Słowa kluczowe: rdzenie transformastorowe, straty mocy, filtry EMI.

Introduction

It has been broadly recognized that the disturbance at the output of the pulse width modulation (PWM) inverters, due to the common mode (CM) voltage, dramatically affects the reliability of the motor.

Motor bearings suffer for the CM inverter-induced currents leading to a reduction of their lifetime; this problem is particularly serious in induction motors often adopted for their robustness [1]-[2]. Among the proposed solutions for increasing the motor reliability, those based on the active compensation of the CM voltage at the motor terminals are particularly effective. Indeed, the CM active EMI filters strongly reduce the CM voltage at the motor terminals so the cause for arising of shaft voltage and bearing currents is eliminated [3]-[5]. Moreover, the use of such a filter scheme gives some benefits on the conducted EMI through the supply line, as shown in [6].

In order to perform the active compensation of the CM voltage, three fundamental steps are necessary: a) the CM voltage detection; b) the transferring of the CM voltage by a transistors amplifier to a common mode transformer (CMT); c) the re-injection of the compensating voltage by the CMT into the power line between the inverter and the motor.

The design of the CMT is a critical issue since, in power applications, it represents the most bulky and costly part of the whole active filter. It also must operate in the frequency range defined by the CM voltage frequency spectrum, managing the magnetic flux due to the drive CM compensation current.

Several recent papers are dedicated to the behaviour of soft magnetic material under non sinusoidal supply; both ferrite and nanocrystalline materials are considered. In particular in [7] the variation of the soft-ferrites permeability and power losses with temperature is investigated, in [8] new soft magnetic powdered iron composites are studied.

As for nanocrystalline, in [9] the dependence of the losses on high frequency is analysed, [10] proposes a model to describe the electromagnetic behaviour and [11] performs an experimental characterization of losses.

Both ferrite and nanocrystalline are utilized in this paper for the CMT core realization. A comparison in terms of size reductions and material losses under non sinusoidal supply conditions, with the same filtering performance, is done. Experimental results are given.

Common Mode Active Filter

The CM active EMI filter considered in this paper is a feed-forward voltage-sensing voltage-compensating device. A detailed description of the filter design and experimental set up is given in [4], whereas [5] contains a detailed model of the filter formulated in the Laplace domain.

A schematic representation of the active filter within an induction motor drive is shown in Fig. 1.

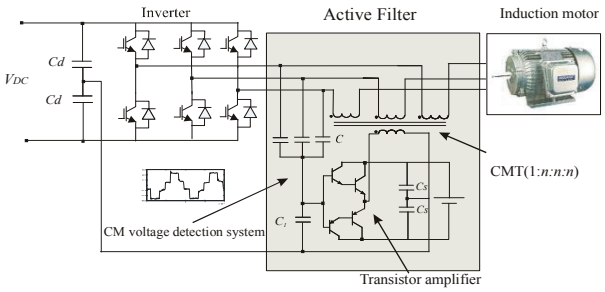

Fig.1. Schematic representation of the CM EMI active filter within a motor drive.

The CM voltage detection system consists of three wye-connected capacitors C and a capacitor C_1, necessary to deliver to the amplifier input a suitable divided CM voltage, v_{CM}/n, where n is the CM voltage partition ratio.

The transistor amplifier is realized by a push-pull emitter-follower circuit with two couple of complementary transistors in Darlington configuration with unitary voltage gain.

The CMT is used to re-inject the common mode voltage with opposite polarity in the three phase line between the inverter and the motor, according to the feed-forward action.

The active filter is applied to an induction motor drive formed of a PWM insulated gate bipolar transistor (IGBT) voltage source inverter (VSI) and a 400V/50Hz three phase induction motor. The inverter maximum current I_{max} is 26 A, the switching frequency f_s is 5 kHz and the induction motor rated power P_m is 0.75 kW.

Design of the CMT

The CMT is realized by four windings on a toroidal magnetic core, the primary has N_1 turns winding connected to the push-pull output and the secondary is composed of three N_2 turns windings series connected to the line

between the inverter and the motor. In order to obtain a correct operation, the following requirements have to be complied: 1) saturation has to be avoided; 2) a unique layer of turns around the magnetic core has to be set up; 3) a turn ratio $N_2/N_1=n$ as high as possible, consistently with the toroidal core size, has to be chosen; 4) a magnetic core material with a suitable bandwidth has to be chosen.

These requirements are explained in the next subsections. Moreover a miniaturization of the whole device, including the CMT, is desired in order to obtain a high power/weight ratio.

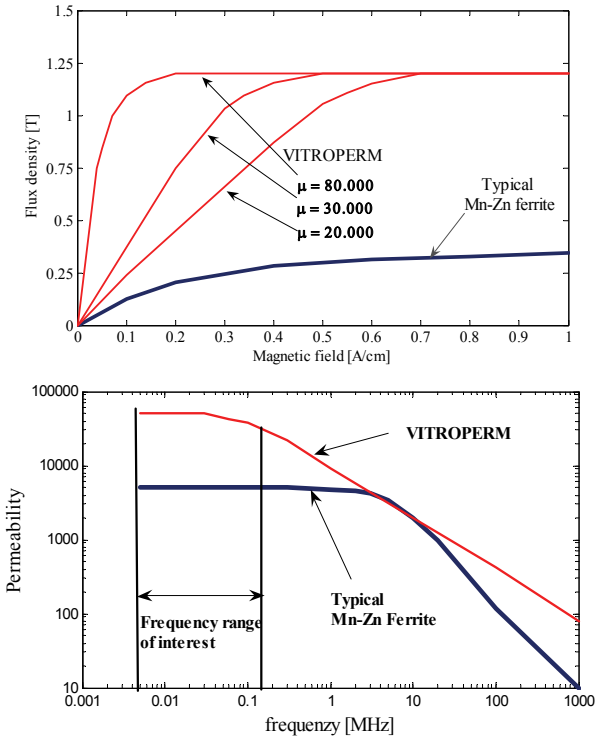

Fig. 2. Magnetization characteristics of the VITROPERM 500F, in comparison with a typical Mn-Zn ferrite (upper) and frequency response of VITROPERM permeability in comparison with a typical Mn-Zn ferrite (lower).

A. Magnetic Material of the Core

The requirement to avoid saturation guarantees the good transfer, without waveform deformation, of the compensating CM voltage to the motor terminals. The general requirements for magnetic materials used in AC applications are satisfied by the typical properties of a soft magnetic material, i. e., high permeability μ and saturation flux density B_s and low coercitivity H_c and power losses P [9], [10], [11]. Among magnetic materials with excellent soft magnetic properties, there are the nanocrystalline, widely used for high frequency applications. In Fig. 2 a comparison between the magnetization characteristics of a nanocrystalline material, the VITROPERM 500F, and of a typical Mn-Zn ferrite is shown [13]. The very high values of the magnetic permeability/section core ratio (A_L) and B_s of nanocrystalline materials allow very high inductance values to be obtained with a reduced section of the core and number of turns. This leads also to low copper losses and small winding capacitance which gives improved high frequency performance. Both ferrites and nanocrystalline materials exhibit a nearly constant magnetic permeability in the frequency range defined by the harmonic content of the CM voltage (starting from the inverter switching frequency, equal to 5 kHz in the case under study, up to the greatest frequency of the CM voltage of about few hundreds kHz). This property is shown in Fig.2. This property allows the primary winding inductance to be assumed as a constant when a periodical waveform supply is imposed in the frequency range of interest [5].

B. Windings design

As for windings design, the first constraint is the realization of a unique layer of turns around the magnetic core, because the use of more layers leads to an incorrect operation of the CMT, due to high frequency capacitive coupling. A second design issue is to realize a ratio, $N_2/N_1=n$, as high as possible, consistently with the toroidal core size [4].

For given magnetic and geometrical characteristics of the magnetic core, an increase of n corresponds to a decrease of the turn number of the primary winding. This limits the increase of n because a reduction of the primary turns results in a decrease of the primary inductance which implies a higher magnetizing current to be delivered by the transistor amplifier.

Imposing a linear operation, it is possible to define the primary and secondary inductance of the CMT, as explained hereinafter.

Integrating the constitutive equation of an N turns inductor, $v(t)=Ldi(t)/dt$ in half a period of the CM voltage $T_s/2=1/2f_s$, in the worst case operation (i.e. square-wave operation), the minimum turns number for the primary can be obtained by the relation [4]:

$$N_1 > \frac{V_{DC} T_S}{2 \cdot 2n \cdot B_s \cdot m \cdot S} \tag{1}$$

where V_{DC} is the DC link voltage, S is the core section and m is the number of cores. Therefore the choice of N_1 and N_2, for obtaining a maximum turns ratio n, is linked to the following conditions: primary turns number according to (1); minimum weight and dimensions of the core, consistently with the set-up of one layer of turns on the core. The CMT primary and secondary windings inductances L_i (i = 1, 2) are given by:

$$L_i = mA_L N_i^2 \tag{2}$$

where A_L is the magnetic permeability/section core ratio.

It is important to note that the minimum primary turns number must be compatible also with the rated current of the complementary transistors of the push-pull output stage.

C. Comparison of different arrangements

Two CMTs have been designed and set up using different magnetic materials for the core: a) N30 Mn-Zn ferrite; b)VITROPERM 500F nanocrystalline material. The magnetic and geometric characteristics of N30 ferrite and VITROPERM 500F cores are reported in Table I.

The design has been carried out so to achieve the same performance in terms of common mode voltage cancellation. Using both the materials, (1) can be fulfilled with the number of primary turns N_1=8 and N_2 turns number is 40. The corresponding turns ratio $N_2/N_1=n$ is equal to 5. On the other hand for the adopted N30 ferrite three cores are necessary against only one for the VITROPERM 500 F.

Table I. Comparison of different magnetic cores characteristics

Parameter	Symbol	Ferrite N30	VITROPERM
Toroidal core size		100x65x15 mm	134.5x95x28.5 mm
Effective section	S	267,2 mm^2	274 mm^2
A_L value	A_L	4.÷6.8μH,10KH	19÷36.8μH, 10 kH
Saturation flux density	Bs	0.45 T	1.2 T
Resistivity	ρ	0.5 Ω·m	0.115 Ω·m
Cores number	m	3	1

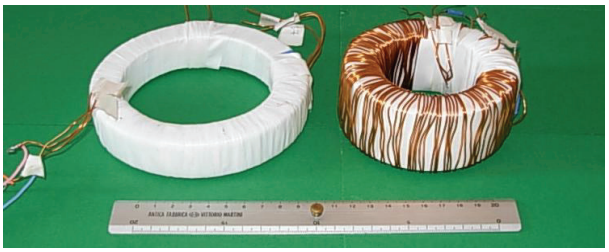

Fig. 3. The two realizations of the CMT: VITROPERM core on the left; N30 ferrite core on the right.

In fig. 3 the two built CMTs corresponding to the two studied configurations are shown.

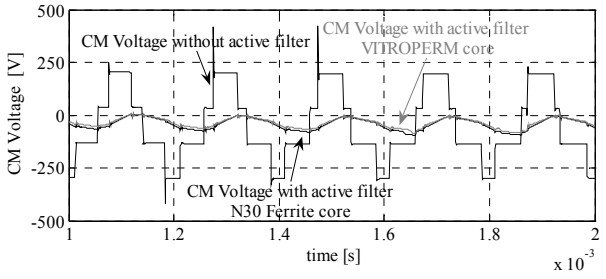

Fig. 4 Measured effect of the active filter on the CM voltage at the motor terminals.

In Fig. 4 the measured CM voltages at motor terminals using the two adopted materials for the core, superimposed with the uncompensated CM voltage, are drawn. The figure shows the effectiveness of the active compensation device.

The filtered CM voltage is practically the same using both the transformers.

The use of a ferrite core implies an increase of the CMT weight of about 27% and an increase of the CMT volume of about 24%. As far as the cost is concerned, the two described realizations are comparable.

A further comparison can be done with respect to the power losses in the magnetic materials.

CMT core material losses

In a range of frequency up to 100 kHz, for a soft magnetic material, the losses, P_{mat}, due to an applied variable magnetic field, can be separated into three main contributions (hysteresis P_H, eddy current P_{ec} and excess losses P_{ex}) [9], [14], according to (3).

$$P_{mat} = P_H + P_{ec} + P_{ex} = a f B^x + b f^2 B^2 + e f^{3/2} \left(B\right)^{3/2} \quad (3)$$

where B is the peak value of the flux density, f is the frequency of the magnetic field, a, b and e are coefficients dependent on the material and x is the Steinmetz coefficient.

When the supply voltage is sinusoidal, if no saturation occurs, the total power lost in the material is:

$$P_{mat} = \frac{1}{2} E_1 \cdot I_1 \cdot \cos(\varphi) = \frac{1}{2} \frac{N_1}{N_2} E_2 \cdot I_1 \cdot \cos(\varphi) \quad (4)$$

where E_1 and I_1 are the peak value of the emf and of the current at the primary winding respectively and φ is their phase displacement angle. However E_1 is not directly measurable because the measured voltage at the primary contains a term due to joule losses of the winding, so the emf measured at the secondary E_2 is used, according to the second part of (4).

A scheme of the measurement system is shown in Fig.5. Particular care must be paid in the evaluation of the displacement angle φ since the absolute error in the evaluation of P_{mat} is strongly dependent on φ that is near to $\pi/2$. Such an absolute error can be expressed as:

$$\Delta P_{mat} = \left|\frac{\partial P_{mat}}{\partial \varphi}\right| \Delta\varphi \cong \frac{1}{2}\frac{n_1}{n_2} E_2 \cdot I_1 \cdot \Delta\varphi \quad (5)$$

The approximation is due to the value of φ near to $\pi/2$.

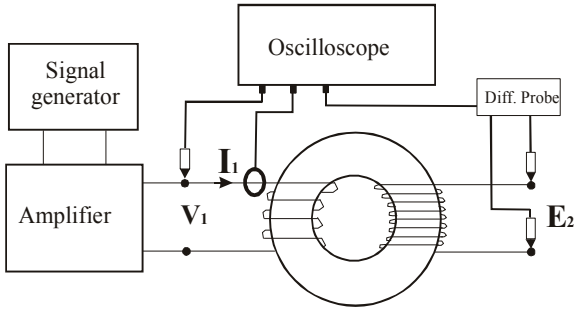

Fig. 5. Scheme of the measurement system.

The magnetic induction can be obtained on the basis of E_2. Finally, the coefficients *a*, *b*, *e* and *x* can be obtained by measuring P_{mat} for several values of *f* and applying a best fitting algorithm on (3). If the *e* coefficient is negligible, (3) can be rewritten as:

$$P_{mat} = P_H + P_{ec} = afB^x + bf^2B^2 \quad (6)$$

For an arbitrary alternate supply waveforms, the losses can be obtained as:

$$P_{mat(sq)} = \alpha^x P_H + \beta^2 P_{ec} \quad (7)$$

where α is given by the ratio of the average value of the rectified waveform and the average value of the rectified value of its fundamental harmonic, and β is the ratio of the root mean square of the supply waveform and the root mean square value of its fundamental harmonic [14]-[15]. For a square wave α=1.23 and β=1.11.

The adopted measuring system is composed of a signal generator HP8648B, a power amplifier PRANA AP32DR180 and a digital oscilloscope Agilent MSO6104A.

The signal generator is connected to the power amplifier so to obtain the desired value of the current amplitude at the CMT primary winding in operating condition; the required current is measured by a current probe Agilent 1147A and the emf voltage at the secondary is obtained by a high voltage differential probe Agilent N2772A [10], [11].

The displacement angle between E_1 and I_1 is given by the oscilloscope, as a delay.

The losses have been firstly evaluated through (4) in sinusoidal supply condition for both ferrite and nanocrystalline materials.

The current amplitudes, giving the magnetic induction corresponding to the operating conditions of the CMT at a frequency of 5 kHz (equal to the carrier frequency of the inverter) and its harmonics, have been used. These values (peak to peak) are I_1=1.03A with a supply voltage V_1=116 V using the ferrite core, I_1=0.8 A with a supply voltage V_1=106 V using the VITROPERM core.

Several measurements of P_{mat}, at different values of *f*, have been performed to find the coefficients of (3). In the considered study the best fitting algorithm gives $e \approx 0$, so (6) can be used. Then the obtained values of P_H and P_{ec} have been weighted as in (7) and the total lost power in the square wave case, that corresponds to the worst case, is obtained.

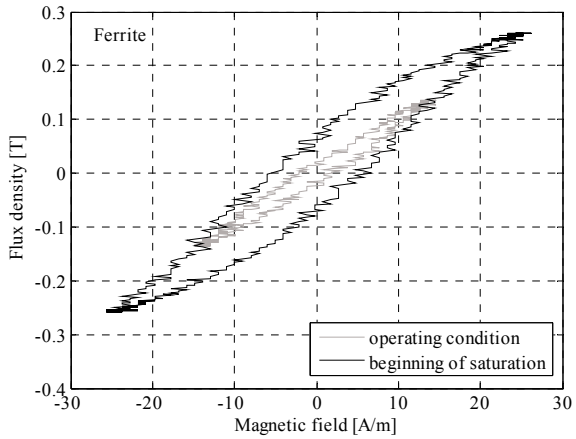

Fig. 6. Hysteresis loop for the ferrite core under operating conditions and in saturation.

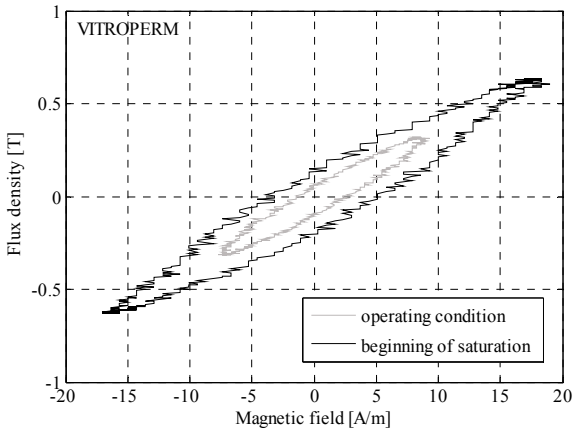

Fig. 7. Hysteresis loop for the VITROPERM under operating conditions and near to saturation.

Figs. 6 and 7 show the hysteresis cycle for the ferrite and for the nanocrystalline material, respectively. Both figures are superimposed with the hysteresis cycles which correspond to the beginning of saturation.

It should be noted that both materials are in the linear zone of operation.

Losses values obtained with sinusoidal and square wave waveforms are reported in Table II.

It should be observed that the value of the power losses in the CMT does not depend on the motor rating current. Therefore the greater is the motor size the smaller will be the influence of these losses on the whole electrical drive efficiency.

Table II. CMT core material losses

Supply	Material	Total [W]	Hysteresis [W]	%	Eddy curr.[W]	%
Sinus.	Ferrite N30	2.83	1.86	64	0.96	36
	VITROPERM.	3.46	1.90	55	1.56	45
Square	Ferrite N30	3.95	2.76	70	1.18	30
	VITROPERM	4.74	2.81	59	1.92	41

Conclusions

In this paper the issues related to the appropriate design of the common mode transformer in CM EMI active filters for electrical drives are analysed. The attention has been focused on the performance of the magnetic material of the CMT core and on the evaluation of its power losses.

Two realizations of the CMT with a ferrite and a nanocrystalline core, respectively, are compared, both giving the same active filter performance. The cost of both transformers are comparable.

Using the nanocrystalline core, the power losses have the same order of magnitude of those observed with the ferrite core despite the higher resistivity exhibited by the ferrite. On the other hand, with the ferrite core, the CMT weight and volume are increased. Therefore the nanocrystalline core-based solution allows a more compact construction and a favourable power/weight ratio.

REFERENCES

[1] G. L. Skibinski, R. J. Kerkman, D. W. Schlegel, “EMI Emissions of Modern PWM AC Drives”, IEEE Ind. Electron. Magaz., Nov./Dec. 1999 pp.47-81.

[2] A. Muetze, A. Binder, “Pratical Rules for Assessment of Inverter-Induced Bearing Currents in Inverter-Fed AC Motors up to 500 kW”, IEEE Trans. Ind. Electron., vol. 54, no. 3, Jun. 2007 pp.1614-1622.

[3] S. Ogasawara, H.Ayano, H. Akagi, “An Active Circuit for Cancellation of Common-Mode Voltage Generated by a PWM Inverter”, IEEE Trans. Pow. Electron., vol.13, no.5, Sep. 1998 pp.835-841.

[4] M. C. Di Piazza, G. Tinè, G. Vitale, “An Improved Active Common Mode Voltage Compensation Device for Induction Motor Drives”, IEEE Trans. Industr. Electron., vol. 55 no. 4, Apr. 2008, pp. 1823 - 1834.

[5] M. C. Di Piazza, G. Vitale, “A Laplace Domain Modelling Approach for CM Active EMI Filters”, PRZEGLĄD ELEKTROTECHNICZNY (Electrical Review), R. 86 NR 3/2010, Page(s): 200-204.

[6] M. C. Di Piazza, A. Ragusa, G. Vitale, “Input EMI in Inverter-fed Motor Drives with Active Filtering of Motor CM Voltage”, Przegla ElektrotechnicznyY (Electrical Review), R. 85 NR 10/2009, Page(s): 248-252.

[7] F. Fiorillo, C. Beatrice, M. Coïsson, L. Zhemchuzhna, “Loss and permeability dependence on temperature in soft ferrites”, IEEE Trans. Magn., Vol. 45, n. 10, Oct. 2009, pp.4242-4245.

[8] P. Marketos, J.P. Hall, S. E. Zirka, “Power loss measurement and prediction of soft magnetic powder composites magnetized under sinusoidal and non sinusoidal excitation”, IEEE Trans. Magn., Vol. 44, n. 11, Nov. 2008, pp. 3847-3850.

[9] Waseem A. Roshena, “Magnetic loss in ferrites”, Journal of applied physics, 101, 09M522 (2007).

[10] P. Sergeant, L. Duprè, “Modelling the electromagnetic behaviour of nanocrystalline soft material”, IEEE trans. Magn. Vol. 45, n. 2, Feb 2009, pp 678-686.

[11] W. Shei, F. Wang, D. Boroyevich, C. Wesley Tipton IV, “Loss characterization and calculation of nanocrystalline cores fog high frequency magnetics applications”, IEEE trans. Power Electronics, vol. 23, n.1 Jan 2008.

[12] H. Y. Lu, J. G. Zhu S. Y. R. Hui, “ Measurement and modeling of thermal effects on magnetic hysteresis of soft ferrites”, IEEE Trans. Magn., Vol. 43, n. 11, Nov. 2007, pp. 3952-3960.

[13] Nanocrystalline Vitroperm EMC Components, VACUUMSCHMELZE GmbH & Co. KG, Hanau, 2004 [Online]. Avaliable:http://www.vacuumschmelze.de/dynamic/docroot/me dialib/documents/broschueren/kbbrosch/PKB_EMV_E.pdf.

[14] A. Boglietti, A. Cavagnino, M. Lazzari, M. Pastorelli, “Predicting iron losses in soft magnetic materials with arbitrary voltage supply: An Engineering Approach”, IEEE Trans. Magn. vol. 39, no. 2, Mar.2003 pp.981-989.

[15] A. J. Moses, “Power loss of non oriented electrical steel under square wave excitation”, IEEE Trans. Magn. vol. 37, no. 4, Jul. 2001 pp.2737-2739.

***Authors**: dr eng. PhD. Maria Carmela Di Piazza, Consiglio Nazionale delle Ricerche, ISSIA sez. Palermo, via Dante, 12 90141 Palermo, ITALY, E-mail: dipiazza@pa.issia.cnr.it; dr eng. PhD. Antonella Ragusa, Consiglio Nazionale delle Ricerche, ISSIA sez. Palermo, via Dante, 12 90141 Palermo, ITALY E-mail: ragusa@pa.issia.cnr.it; dr eng. Gianpaolo Vitale, Consiglio Nazionale delle Ricerche, ISSIA sez. Palermo, via Dante, 12 90141 Palermo, ITALY, E-mail: vitale@pa.issia.cnr.it*

.